

Uncertainty Wedge Analysis: Quantifying the Impact of Sparse Sound Speed Profiling Regimes on Sounding Uncertainty

J. Beaudoin*

J. Hiebert[†]

B. Calder[‡]

G. Imahori[§]

Abstract

Recent advances in real-time monitoring of uncertainty due to refraction have demonstrated the power of estimating and visualizing uncertainty over the entire potential sounding space. This representation format, referred to as an uncertainty wedge, can be used to help solve difficult survey planning problems regarding the spatio-temporal variability of the watercolumn. Though initially developed to work in-line with underway watercolumn sampling hardware (e.g. moving vessel profilers), uncertainty wedge analysis techniques are extensible to investigate problems associated with low-density watercolumn sampling in which only a few sound speed casts are gathered per day.

As uncertainty wedge analysis techniques require no sounding data, the overhead of post-processing soundings is circumvented in the situation when one needs to quickly ascertain the impact of a particular sampling regime. In keeping with the spirit of the underlying real-time monitoring tools, a just in time analysis of sound speed casts can help the field operator assess the effects of watercolumn variability during acquisition and objectively seek a watercolumn sampling regime which would balance the opposing goals of maximizing survey efficiency and maintaining reasonable sounding accuracy.

In this work, we investigate the particular problem of estimating the uncertainty that would be associated with a particular low-density sound speed sampling regime. A pre-analysis technique is proposed in which a high-density set of sound speed profiles provides a baseline against which various low-density sampling regimes can be tested, the end goal being to ascertain the penalty in sounding confidence that would be associated with a particular low-density sampling regime.

In other words, by knowing too much about the watercolumn, one can objectively quantify the impact of not knowing enough. In addition to the goal-seeking field application outlined earlier, this allows for more confident attribution of uncertainty to soundings, a marked improvement over current approaches to refraction uncertainty estimation.

1 Introduction

Uncertainty propagation allows for the estimation of the horizontal and vertical uncertainty of a depth sounding based on

- the uncertainties of all additional measurements made in support of the sounding, and
- a mathematical model that describes the relationship between the uncertainties of the supporting measurements and the uncertainty of the reduced sounding.

The total propagated uncertainty (TPU) of a sounding results when one uses the mathematical model to estimate how the uncertainties of observed parameters combine to affect the uncertainty of sounding.

Although attribution of uncertainty to a sounding is a noble effort in and of itself, it has proved to be useful for many applications in hydrography, particularly in automated data validation and filtering [5]. TPU estimates are also often used to reject data whose TPU exceeds a specified tolerance [15]. Manufacturers of mapping instrumentation strive to maintain sensor accuracies within tolerable limits to minimize impact on TPU. There is clearly merit in having the TPU as accurate as possible. This hinges on having (a) reasonable estimates of the uncertainties of the supporting measurements, and (b) an accurate uncertainty propagation model.

A weakness in many uncertainty models is the treatment of the spatio-temporal variability of the watercolumn. For example, the Hare-Godin-Mayer [9] model combines the effects of sound speed instrumentation

*Ocean Mapping group, University of New Brunswick, Fredericton, NB, Canada

[†]NOAA Hydrographic Systems and Technology Program, Silver Spring, MD, USA

[‡]Center for Coastal and Ocean Mapping and NOAA-UNH Joint Hydrographic Center, University of New Hampshire, Durham, NH, USA

[§]NOAA Office of Coast Survey, Silver Spring, MD, USA

uncertainty and spatio-temporal variability of the water column into a single uncertainty estimate. The same model also limits the sound speed uncertainty effect to the deviation in refracted ray angle at the interface of a two layer model of the ocean.

Sound speed instrumentation uncertainties are typically available from instrument manufacturers or can be estimated based on observed instrument drift or from repeated casts. The effect of systematically biased sound speed instrumentation has been investigated by several researchers and is relatively well understood [7, 8]. Uncertainty due to spatio-temporal watermass variability, however, is markedly different in nature from that of instrumentation uncertainty and can potentially lead to large sounding biases if the watermass variability is inadequately sampled.

As with instrumentation uncertainty, the random small-scale variations throughout the watercolumn tend to have a negligible effect, but systematic large scale variations can lead to significant biases, with the nature of the bias varying dramatically with the vertical location and nature of variability in the water column. Applying a single sound speed uncertainty value for the entire watercolumn likely remains a valid approach for instrumentation uncertainty, however, this may not suffice for spatio-temporal variability as the vertical location of the variability in the watercolumn has a strong modulating effect on the magnitude of refraction artifacts. It is only those soundings that are deeper than the water column variability that are impacted by the variability. For example, consider the set of sound speed casts in Figure 1 where variability is pronounced between depths of 3 to 13 m. Though the variability may be dramatic, it is of little consequence for those soundings shoaler than 3 m. In this case, a single all-encompassing uncertainty value for the speed of sound that applies to all depths could produce overly pessimistic or overly optimistic estimates of sounding uncertainty, depending on the sounding’s depth with respect to the depth of the water column variability.

Recent work within NOAA has attempted to simplify the task of estimating the component of TPU due to variable watercolumn conditions. The Estimating Sound Speed uncertainty (ESS) method is based upon a comparison of raypaths associated with a pair of synthetic sound speed casts statistically derived from a set of observed casts [10]. This work was an important step forward for two reasons. Firstly, it provided an objective method to calculate the sound speed uncertainty from a set of observed casts, a process that was previously very subjective. The second, and perhaps more important impact, was that it allowed field operators to objectively quantify the impact of varying

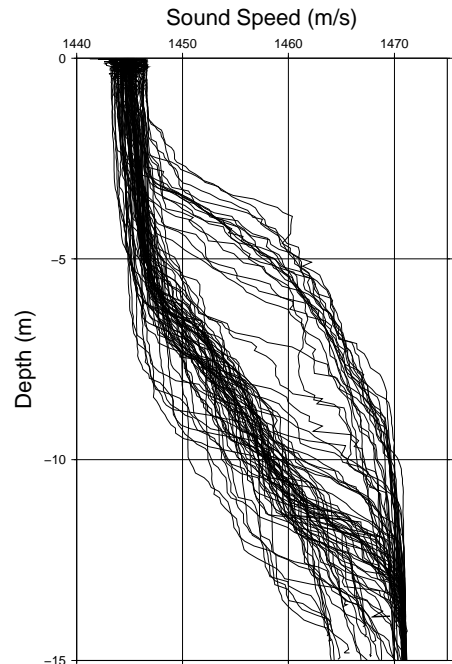


Figure 1: Sound speed casts gathered over a 2.5 hour interval near the mouth of the Rotterdam Waterway in March 2009.

watercolumn conditions in the field, e.g. [17]. As the ESS method was designed to generate uncertainty estimates to the Hare-Godin-Mayer model as implemented in the CUBE algorithm [5], its applicability was limited in that it still reduced watercolumn variability to a single uncertainty value. Additionally, the underlying assumption that variability at the surface is perfectly correlated with variability at depth limits its use to a very limited set of oceanographic environments. These types of conditions are seen, for example, in very well mixed environments where the temperature and salinity are more or less constant over the watercolumn and change as a whole due to spatial or temporal variations.

Similar work done independently at the University of New Brunswick (UNB) has demonstrated the value of estimating and visualizing the uncertainty due to differing watercolumn conditions over the entire potential sounding space, i.e. from sounder to seafloor and across the entire angular sector. Through a comparative raytrace simulation process [3], uncertainty is estimated over the potential sounding space, generating what we refer to as an “uncertainty wedge” [1]. In this work, the UNB method is used to (a) quantify the impact of observed variability in terms of sounding

uncertainty, and (b) analyze sounding uncertainties associated with various sampling regimes, e.g. sampling only once per day.

Fundamentals of uncertainty wedge calculation and analysis are discussed first, followed by examination of sample problems which demonstrate the application of uncertainty wedge analysis techniques to common types of problems in hydrographic surveying. Finally, the issue of integrating uncertainty wedges, and the analysis techniques described herein, into existing algorithms and workflows is discussed.

2 Method

As mentioned earlier, the UNB method is to simulate what sounding uncertainty would result from the use of alternate models of the watercolumn. The simulator requires only sound speed profiles as input and can be tuned to match any mapping system. Variable parameters include draft, angular sector, range performance envelope, and the inclusion of surface sound speed probe as an additional measurement (though surface sound speed probe data are not required). Appendix A discusses these parameters in further detail, Appendix B specifically treats the case of simulating the inclusion of a surface sound speed measurement.

The simulator is based upon monitoring the progression of two or more acoustic raypaths, all sharing a common initial launch, or depression, angle and each raypath being associated with a particular sound speed profile. A constant velocity acoustic raytracing algorithm [14] is used to explore how differing models of the sound speed structure, e.g. the two sound speed profiles shown in Figure 2, can alter the raypath, and ultimately, the divergence of the set of raytraced solutions for a given two-way travel-time (TWTT) and depression angle, as shown in Figure 3. By systematically modifying the depression angle and TWTT, the entire potential sounding space is explored to populate a depth and distance indexed table of sounding depth and horizontal discrepancies, as shown in figures 4 and 5. These tables are referred to as uncertainty wedges throughout the remainder of this work.

The raytrace simulator can be used to track the dispersion of raypaths associated with a set of several sound speed profiles representing a sample of the population of possible water column conditions in a given area. This type of analysis, referred to as a Variability Analysis (VA), allows for the construction of a variability wedge, or a **v-wedge**. The **v-wedge** captures the “potential uncertainty” associated with water mass variability. Figure 6 demonstrates the principle

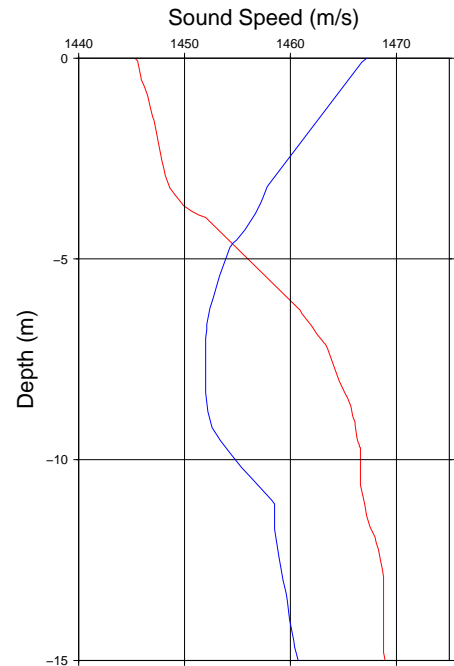


Figure 2: Two sample sound speed profiles.

behind the estimation of the potential horizontal and depth uncertainty for a single location in the potential sounding space. Expanding the analysis for all nodes in the sounding space, one can construct a **v-wedge**. For example, Figure 7 shows a **v-wedge** constructed for the set of sound speed casts shown in Figure 1.

An Uncertainty Wedge Analysis (UWA) consists of comparing two raypaths only, allowing for a quantitative answer to the following question: “What would the bias be if sound speed profile B was used in the place of sound speed profile A?”, where profile A represents known conditions and profile B represents an alternate model whose fitness is to be tested by a comparison to A. As the comparison of two casts quantifies the sounding bias that would be introduced if one cast had been used in the place of the other, the resulting uncertainty wedge is more aptly named a bias wedge, or a **b-wedge**. By comparing many pairs of casts, a set of **b-wedges** can be generated; these can then be averaged to provide a mean bias wedge along with a standard deviation wedge. These are respectively referred to as an **m-wedge** and **s-wedge** in this text. By modifying the casts that are used as reference and/or those that are used as test candidates, one can perform sophisticated analyses. For example, one can test the fitness of an oceanographic climatology as

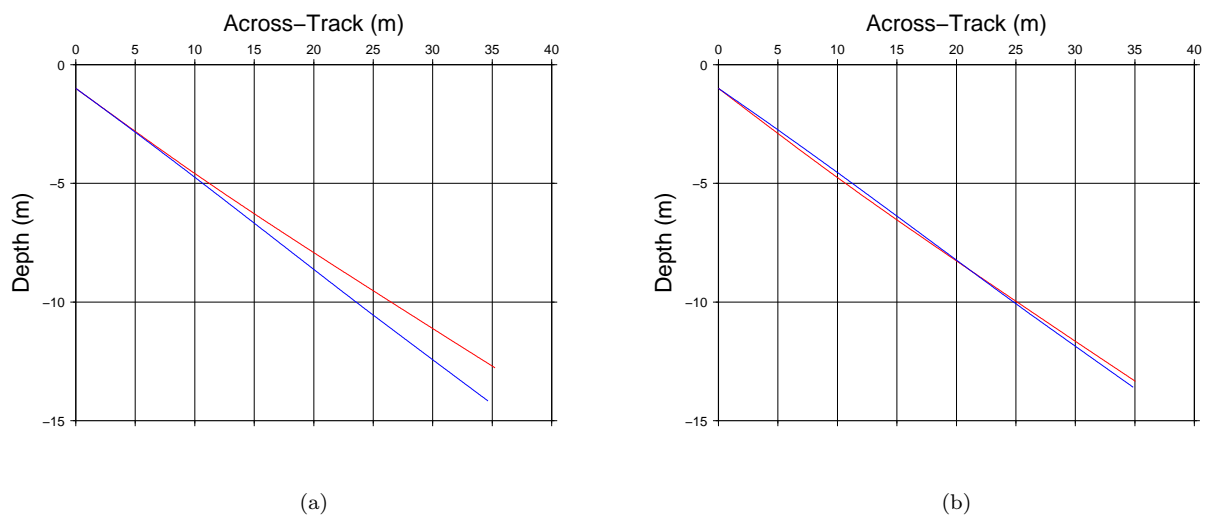


Figure 3: Raytrace solutions associated with sound speed casts in Figure 2; draft is 1.0 m, depression angle of 20° and TWTT is 0.051 s. The raytraces in Panel A demonstrate how dramatic variations in the watercolumn can cause great divergence in the raypaths. Panel B demonstrates how using a surface sound speed probe has the potential to mitigate the effects of surface variability in some cases. In this latter case, the solutions were computed using a common surface sound speed value of 1455 m s^{-1} .

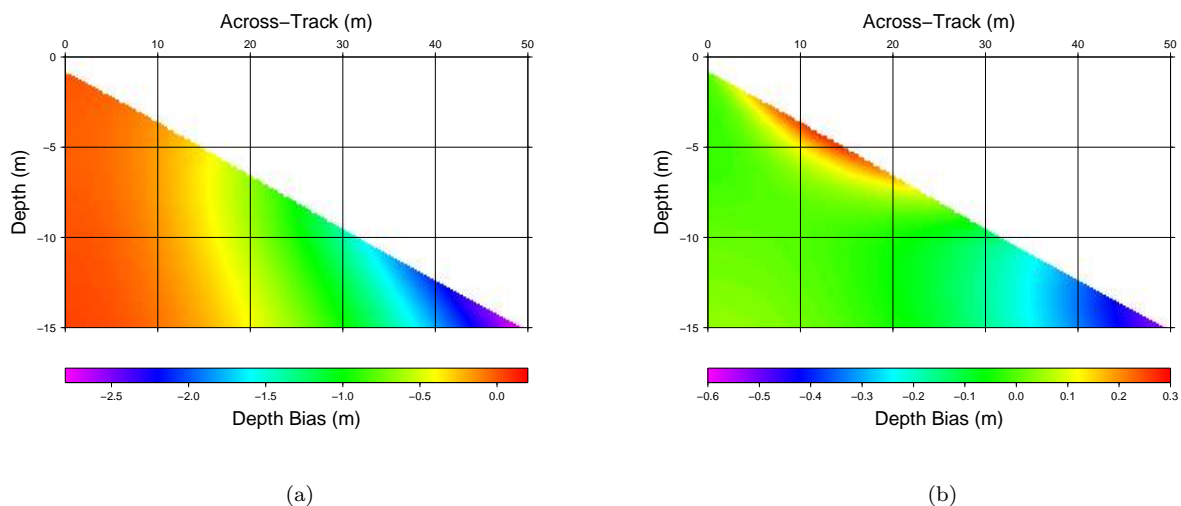


Figure 4: Depth uncertainty wedges associated with casts in Figure 2; draft is 1.0 m and angular sector of 150° . As in Figure 3, Panel A and B show the cases of independent and common surface sound speeds, respectively. Note the different colour scales for each panel.

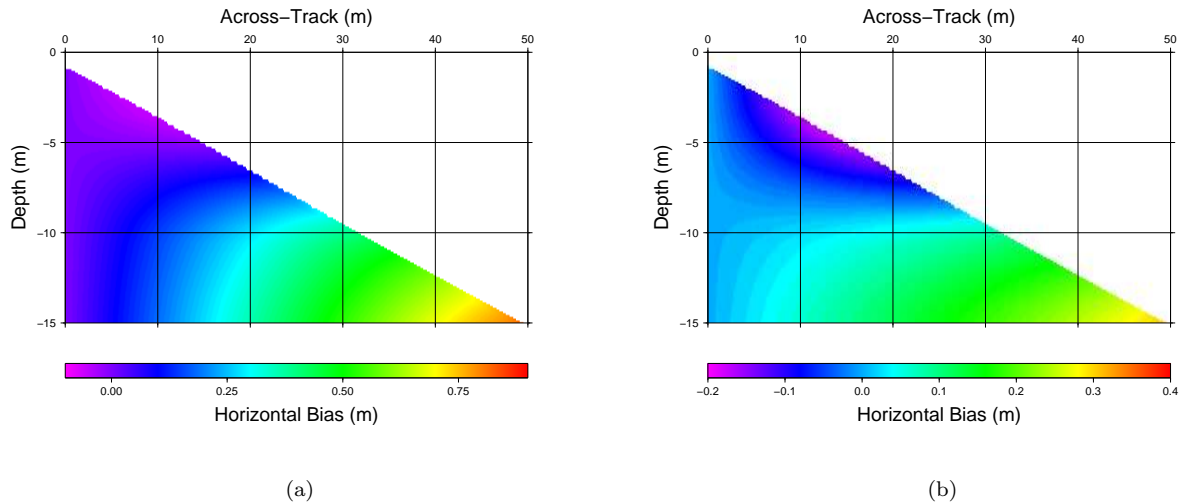


Figure 5: Horizontal uncertainty wedges associated with casts in Figure 2; draft is 1.0 m and angular sector of 150° . As in Figure 3, Panel A and B show the cases of independent and common surface sound speeds, respectively. Note the different colour scales for each panel.

a source of sound speed information, in this case the **s-wedge** represents the potential uncertainty associated with using a climatology [3]. Another example is in real-time monitoring of uncertainty associated with high rate water column sampling, where **b-wedges** are used to ascertain whether or not appreciable changes in the watercolumn are occurring during the interval between casts. If so, the sampling rate is increased until the sounding discrepancy between casts is acceptable or at least within tolerable limits. If not, the operator may choose to relax the profiling rate to reduce wear and limit exposure to risk of grounding or fouling of instrumentation [1].

In summary:

- **v-wedge** (variability wedge): measure of the potential uncertainty associated with the spatio-temporal variability of the water column.
- **b-wedge** (bias wedge): measure of the bias had an alternative cast been used in place of an observed cast.
- **m-wedge** (mean bias wedge): arithmetic mean of several **b-wedges**.
- **s-wedge** (sigma wedge): standard deviation associated with a set of **b-wedges**.

The following section demonstrates how these uncertainty representation formats and analysis techniques can be used to help the hydrographic surveyor achieve their accuracy requirements.

3 Sample Analysis Problems

Time spent on reconnaissance is seldom wasted.

British Army Field Service Regulations, 1912

Much can be learned about water column variability, and its impact on sounding accuracy, by heavily oversampling a water mass using underway or expendable sound speed profiling instrumentation. Using analysis techniques such as those presented in this work allows the hydrographic surveyor to perform an oceanographic pre-analysis of the survey area; insights gained during such an effort can help direct immediate or future field operations.

For example, a VA can quantify the potential uncertainty associated with watermass variability using the entire set of casts collected during such a sampling effort. In the event that the VA shows that the variability will have little impact on sounding accuracy, the data set can be artificially reduced, or thinned, to match a planned operational sampling scheme, e.g., sampling every six hours, to ascertain perhaps how many casts are actually required. UWA techniques can then be used to quantify the uncertainty cost associated with a given sampling regime in light of the potential uncertainty quantified by the **v-wedge**. On the other hand, if the VA shows a potential for appreciable and intolerable uncertainty, the surveyor may choose to sample

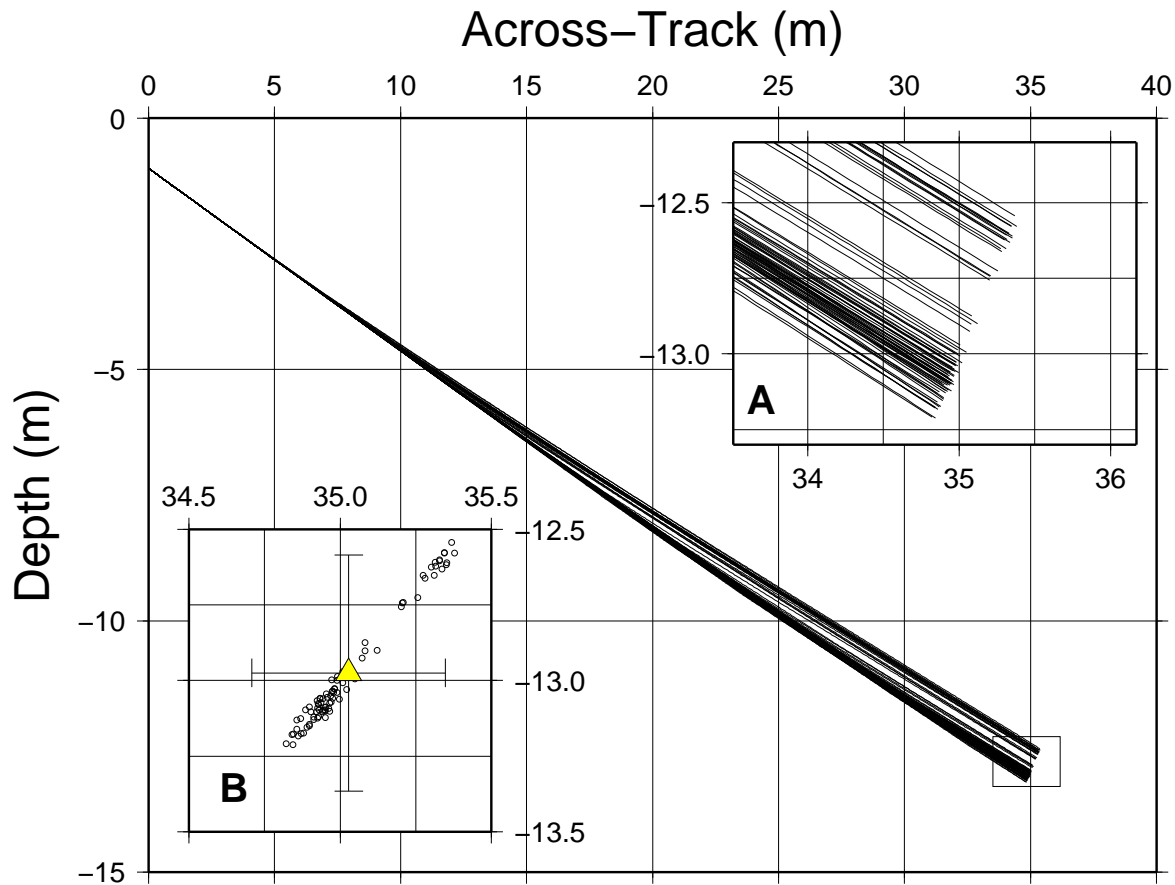


Figure 6: Raypaths calculated for the 82 sound speed profiles shown in Figure 1 using a draft of 1.0 m, a depression angle of 20° , a TWTT of 0.051 s and a common surface sound speed of 1445 m s^{-1} . The inset panel (A) on the upper right corresponds to the rectangular box drawn near the termini of the raypaths shown in the main panel. The lower left panel (B) shows the ends of the raypaths only and demonstrates how the final raytraced solutions disperse depending on which sound speed profile is used for raytracing. The mean depth and position are indicated by the yellow triangle, the error bars indicate the 95% confidence level. Note that the main panel and upper right panel share the same distorted aspect ratio whereas the aspect ratio of the lower left panel is correct.

the watercolumn more often or to accept the loss of accuracy in the outer portions of their mapping swath and reduce their line spacing accordingly. In either case, such a pre-analysis effort allows for a more intelligent, efficient and systematic allocation of survey resources. For example, a launch capable of underway sampling might be sent to areas with dynamic oceanographic conditions whereas launches equipped with standard sound speed sampling equipment can be sent, with confidence, to areas where the oceanography is perhaps more quiescent.

The following sample problems demonstrate the power of such pre-analysis techniques. We begin by performing a VA for a set of locations in an area with

very dynamic oceanography and demonstrate how the pre-analysis can identify problematic areas. This is followed by an UWA in an area where oceanographic changes have little impact on sounding accuracy. In this case the surveyor can ascertain just how few sound speed casts would actually be required to maintain accuracy.

3.1 Variability Analysis

In this section, we demonstrate how **v-wedges** can be used to capture and quantify the spatial and temporal variations of survey area's watercolumn characteristics. In this case, we examine the Rotterdam Waterway in the Netherlands, where the Meuse river meets

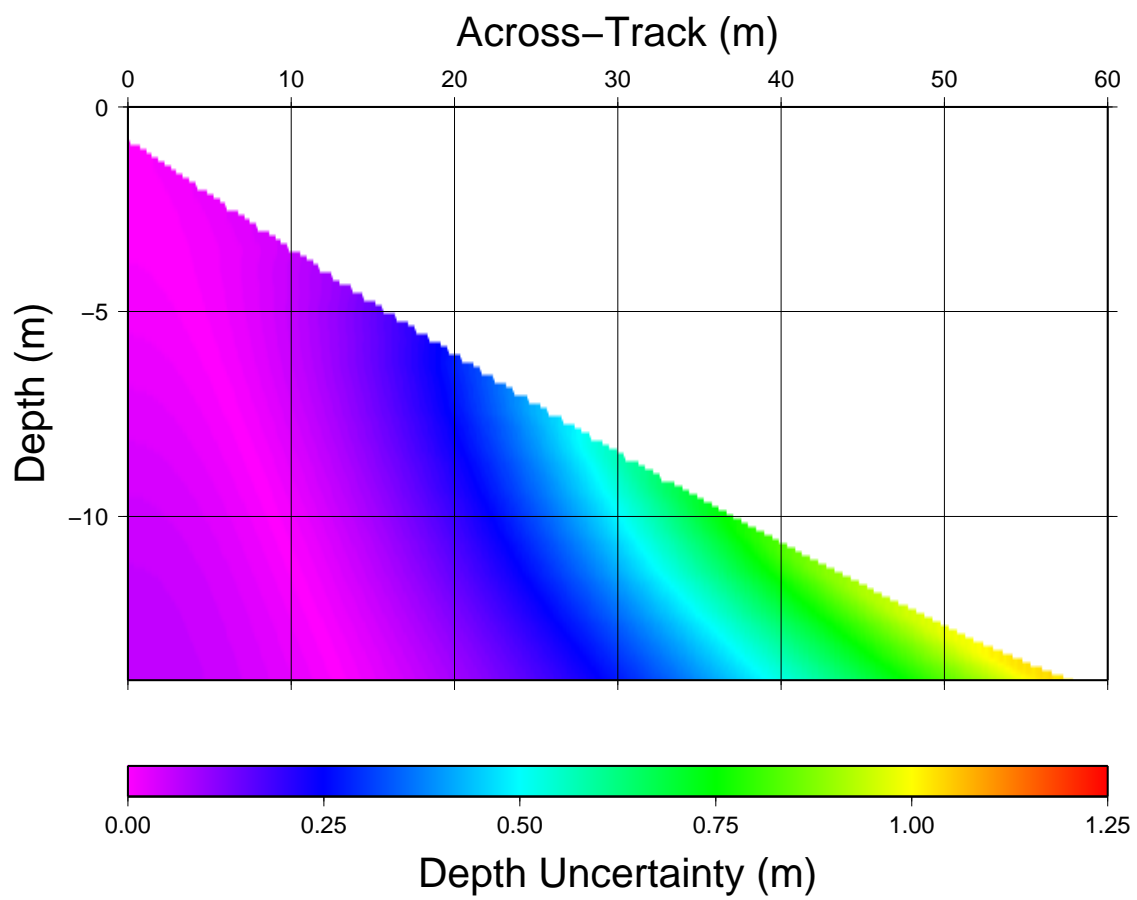


Figure 7: A Variability Wedge generated from the set of sound speed casts shown in Figure 1.

the North Sea (see Figure 8). A field trial was conducted by the Dutch Public Works (Rijkswaterstaat, RWS) in March of 2009 with an ODIM Brooke Ocean MVP30 and a Kongsberg EM3002 (dual-head) multi-beam onboard the RWS survey vessel *Corvus*. This area was selected for the trial, because it tends to suffer from particularly strong refraction artifacts and because high sedimentation rates and heavy vessel traffic necessitate repeated surveys every four weeks.

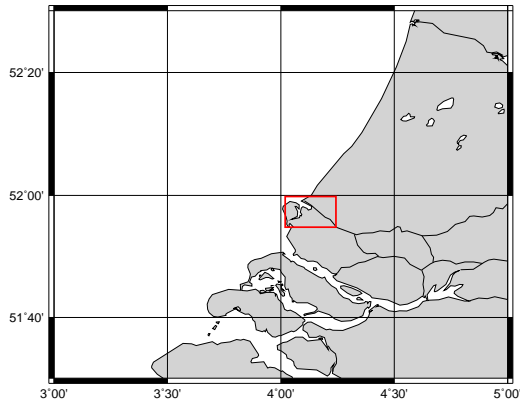


Figure 8: Overview map showing study area at the entrance to the Rotterdam Waterway.

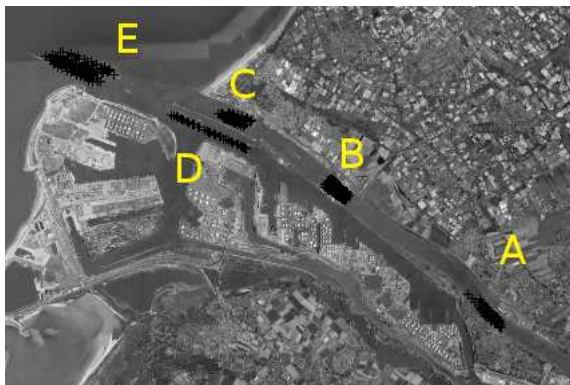


Figure 9: Satellite image of sound speed cast locations in Rotterdam Waterway, March 2009. Data courtesy of Rijkswaterstaat (Dutch Public Works). Cast locations are indicated for several survey areas as black crosses. Text labels correspond to plots in Figures 13 through 17.

Over the course of the seven day trial, 2,151 sound speed casts were acquired in several test survey areas and over long sections running from Maassluis to an area just offshore of the mouth of the Waterway (loc-

tions A and E in Figure 9, respectively). The temperature and salinity variations observed are consistent with a salt wedge type estuary with a strongly stratified watermass. Fast flowing surface water is predominantly fresh and bottom water is predominantly salty with little mixing between the two watermasses. Salt water intrudes upriver on the flood tide, acting like a wedge and sliding underneath the surface fresh water. During a falling tide, strong river currents rapidly flush the salty bottom water back to sea.

These types of environments are challenging to hydrographers as the majority of the variability is in the depth of the interface between the fresh and salt water, with the interfacial depth varying strongly spatially and temporally (note the turbulent interface between the two layers in Figure 10). As the change in sound speed can be quite dramatic at the interface between the fresh and salt water, soundings can refract quite strongly and can lead to significant sounding uncertainty with seemingly small variations in the interfacial depth. Figures 10 through 12 depict the intrusion of saltwater below the freshwater over various stages of the tide for three days of the seven day trial.

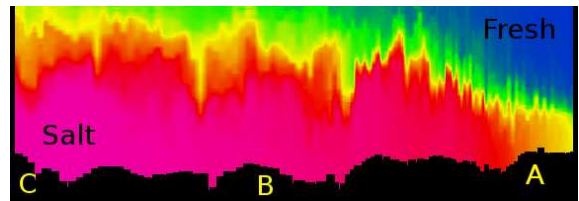


Figure 10: Vertical salinity section (20 m deep) over a distance of 11.5 km from station A to C on March 25th.

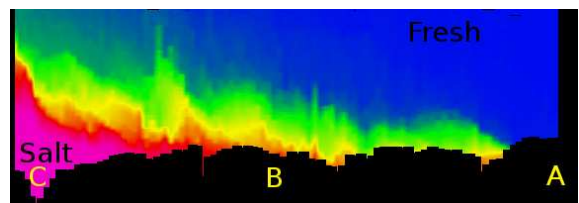


Figure 11: Vertical salinity section from station A to C on March 30th.

Plots of sound speed profiles and **v-wedges** derived from them are shown for locations A through E in Figures 13 through 17, respectively (note that the locations were sampled on different days). Examining location A first (Figure 13), the midwater interfacial depth varies vertically by almost 5 m and introduces significant outer beam uncertainty beyond depths of 5

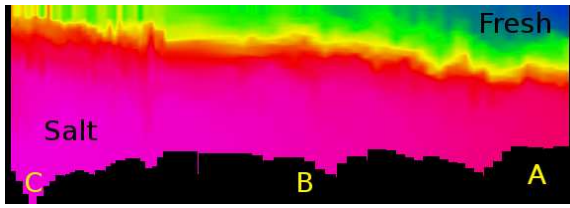


Figure 12: Vertical salinity section from station A to C on April 2nd.

m. Referring to the salinity section in Figure 11, it is clear that there are stages of the tide where the salt water is flushed away. Though the potential uncertainty quantified by the **v-wedge** is non-negligible in for the stage of the tide over which the casts of location A were gathered, a patient surveyor might instead choose to wait for an appropriate stage of the tide before surveying in this area. That is, armed with nothing but a tide table and a conventional sound speed profiling instrument, the surveyor could collect exploratory casts up the river on a falling tide until the terminus of the salt wedge was found. Once found, a survey could proceed slightly upstream of the salt wedge with little concern for the troublesome variability associated with the wedge as it is safely downstream of the survey location and not likely to return until the tide begins to rise after low water.

Turning to location B, the variability is more pronounced and dominates over a larger portion of the watercolumn, perhaps half of the watercolumn as opposed to one third as was observed at location A. The variability is predominantly spatial in nature and results from survey lines running parallel to the river flow, coinciding with the direction of maximum spatial variability. In this case, none of the sections in figures 10 through 12 show location B being free of the effects of the migrating salt wedge. Location B can likely be classified as a “trouble spot” in which underway sampling instrumentation is routinely used for all surveys in the area.

Compared to location A, the variability at location C occurs deeper in the watercolumn. As a result, the potential uncertainty is lower when compared to the **v-wedge** for location A, where the variability occurs much shallower in the watercolumn. One can argue that location B would benefit from this same logic as there are stages of the tide where the variability is much lower in the watercolumn, for example, compare location B in Figure 10 and Figure 10.

The Caland Canal section of the Waterway (location D) is cut off from direct freshwater inflow from the river, it thus suffers less from the refraction prob-

lems that affect surveyors working in the main channel of the Waterway. In this area, it is likely possible to sample once every few hours and still maintain accuracy. Given a fleet of survey vessels, one might assign this site to the vessels equipped with static profiling systems and focus vessels equipped with underway profiling systems in the main river channel.

At the mouth of the river (location E), the outflow of the river is limited to a thin surface layer. As the variability is quite shallow in the watercolumn, the divergence of raypaths occurs early on during raytracing. Sounding uncertainty is thus introduced at a shallow depth and persists over the remainder of the raytrace. In this area, it may be advisable to use a deeper draft vessel. A VA was performed for a deeper draft vessel to demonstrate, the resulting **v-wedge** is shown in Figure 17b. Though there is a loss in swath width associated with the deeper draft vessel, the survey system is much less sensitive to the surface variability. A further advantage to the deeper draft vessel is that surface sound speed instrumentation uncertainties will have less of an effect on electronically beam-formed systems as there is less variability at the transducer depth.

3.2 Sampling Regime Analysis

In this section we examine an MVP data set consisting of 224 casts collected in Advocate Bay in the Bay of Fundy (Canada), by the CCGS Matthew in October of 2008 (refer to figures 19 and 20). For research purposes, the profiling interval was set at two minutes. This rate is much higher than standard acquisition rates onboard the Matthew: casts are typically only collected when significant changes in surface sound speed are observed via the surface sound speed probe. The watercolumn was observed to be completely mixed with temperature and salinity remaining more or less constant with depth, thus the only vertical variation in sound speed was due to the pressure increase with depth. Small spatial variability in the temperature and salinity led to small changes in the sound speed over the survey area (approximately 10 km by 2.5 km), refer to figures 21 and 22. A **v-wedge** has been constructed for the set of casts (Figure 23). Clearly the variability here is not particularly troublesome. Contrasting starkly with the previous pre-analysis problem done for the Rotterdam Waterway, the problem here is instead to identify just how few casts would be required to maintain accuracy.

In this sample problem, a set of **b-wedges** is computed by comparing each cast in the full set of casts (the “truth”) to the profile that would have been used in the artificially thinned set of casts (e.g., the first

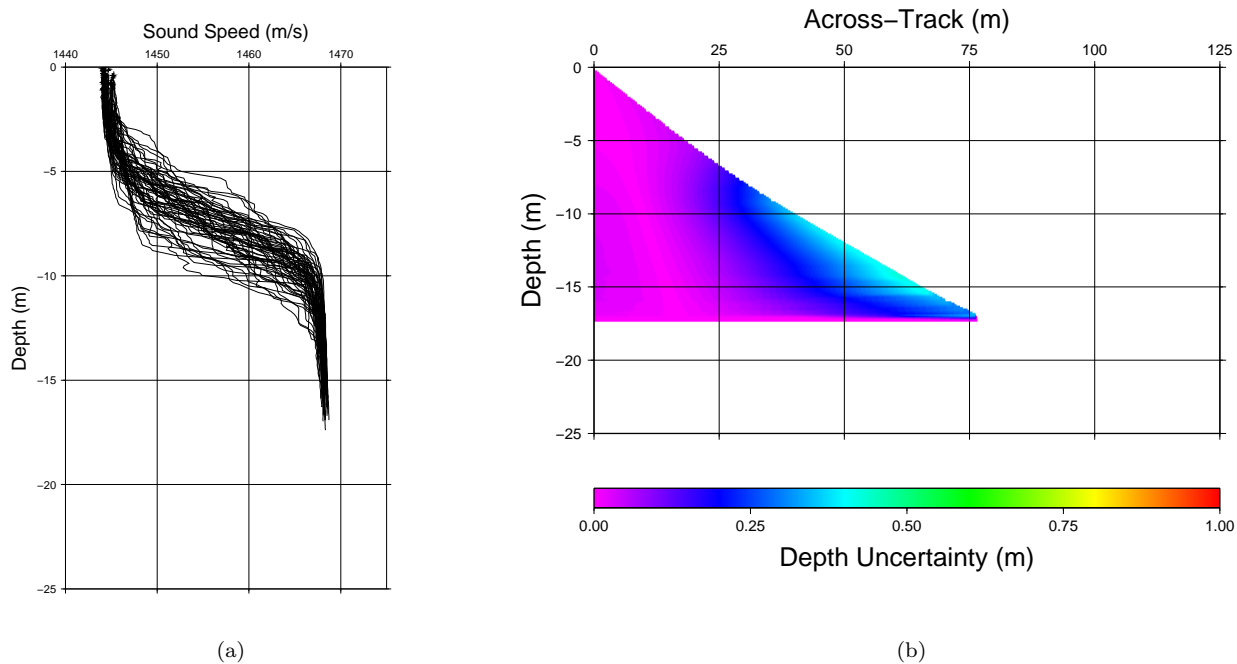


Figure 13: Sound speed casts and **v-wedge** for a 1.5 hour period near Maassluis in the Rotterdam Waterway (60 casts, location A in Figure 9).

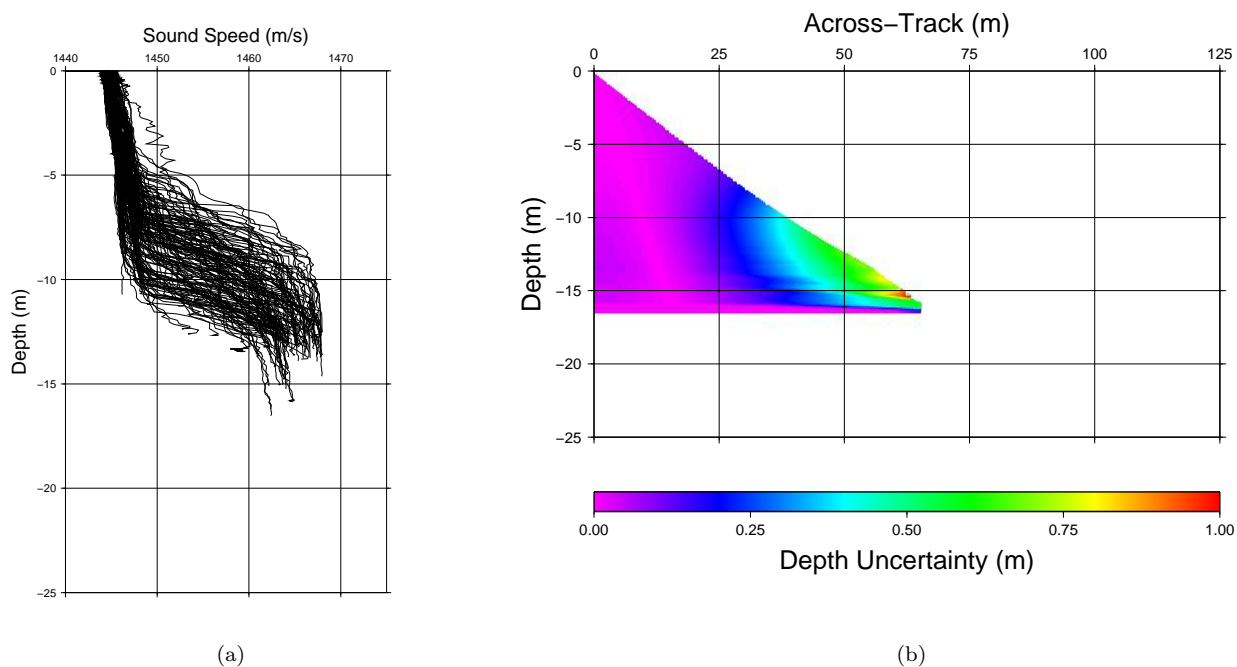


Figure 14: Sound speed casts and **v-wedge** for a 2.5 hour period while surveying within the surge barrier structure of the Rotterdam Waterway (148 casts, location B in Figure 9).

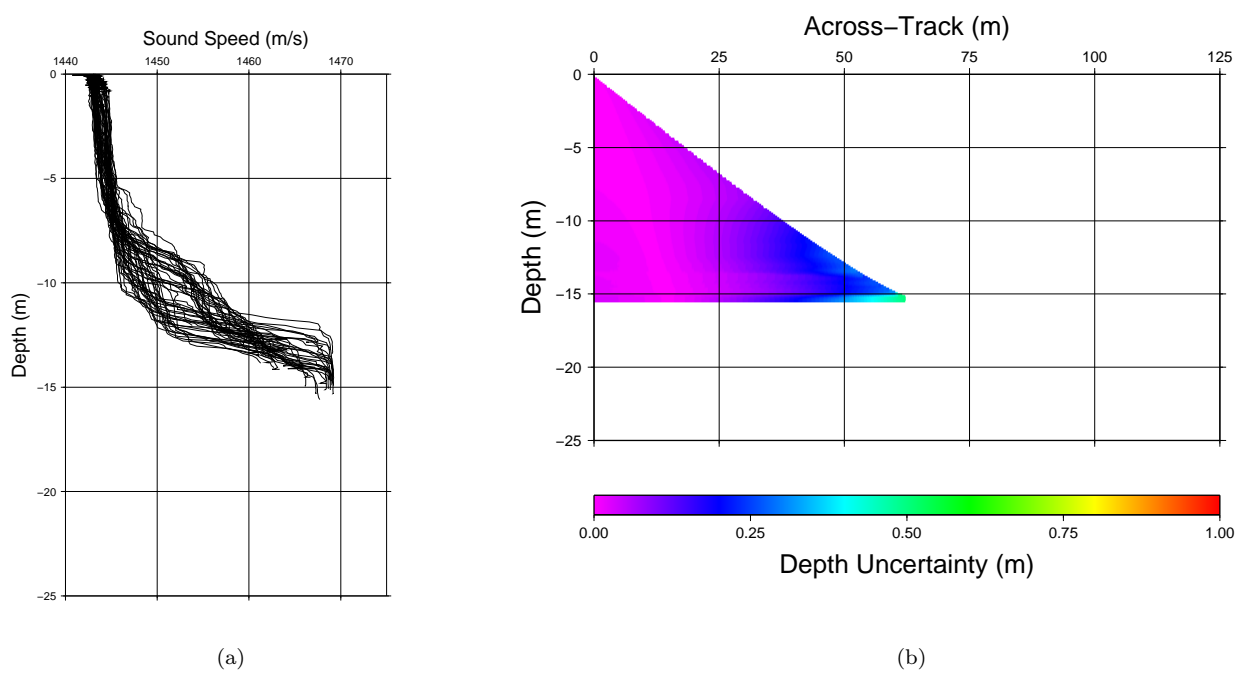


Figure 15: Sound speed casts and **v-wedge** for a 1.0 hour period at the entrance to the Rotterdam Waterway (52 casts, location C in Figure9).

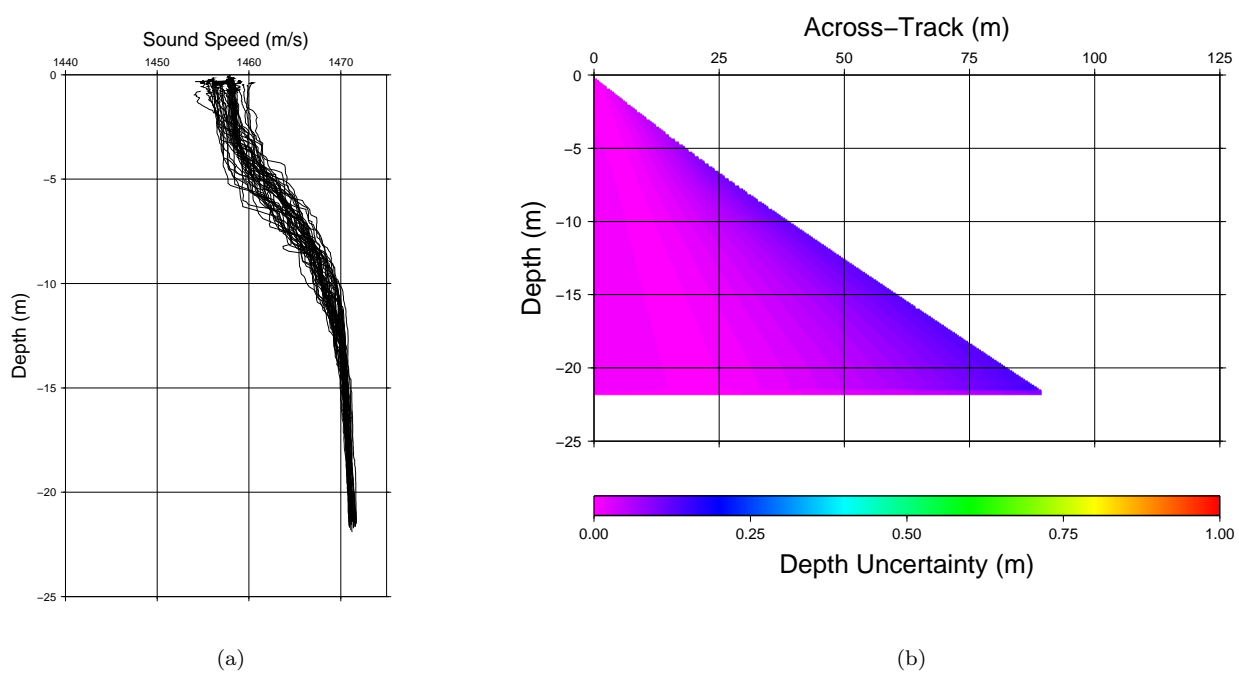
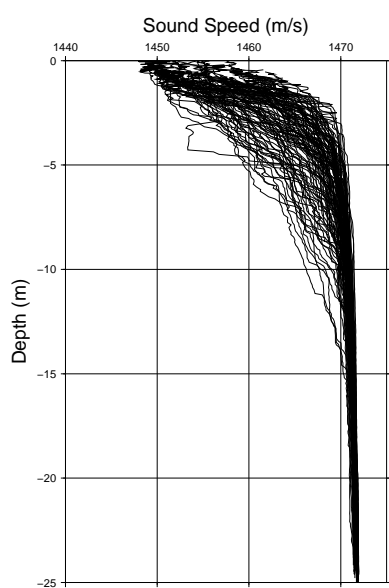
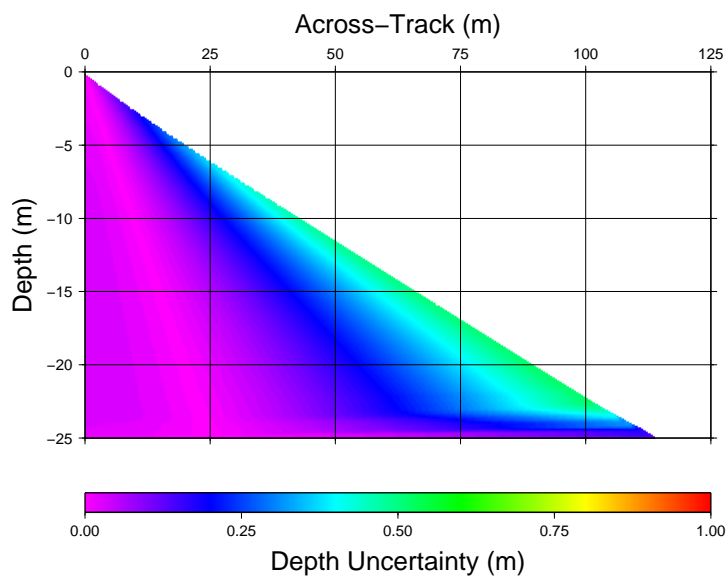


Figure 16: Sound speed casts and **v-wedge** for a 2.5 hour period in the Caland Canal portion of the Rotterdam Waterway (44 casts, location D in Figure9).



(a)



(b)

Figure 17: Sound speed casts and **v-wedge** for a 2.5 hour period just off the entrance to the Rotterdam Waterway (106 casts, location E in Figure9).

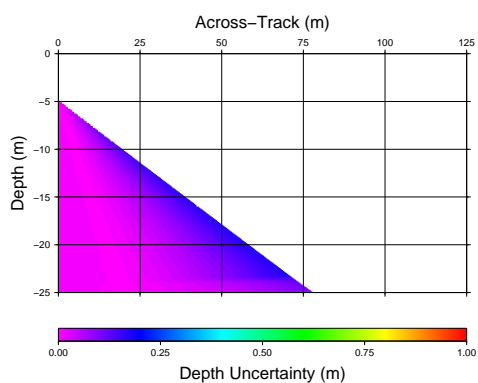


Figure 18: **V-wedge** for a deep draft vessel in Location E, contrast with Figure 17b where a draft of 0.3 m was used.

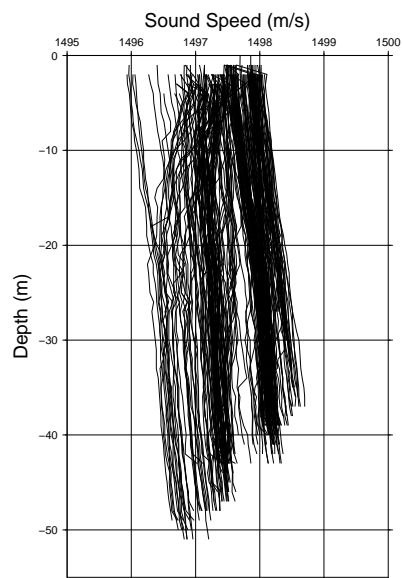


Figure 19: Sound speed profiles acquired by the CCGS Matthew in Advocate Bay (224 casts).

cast of the day, or six casts used with a nearest-in-distance selection algorithm). In this case, pairwise comparisons are made that allow for the compilation of **m-wedges** and **s-wedges** that capture the combined effects of (a) the water column variability, and (b) the simulated sampling regime. It is proposed that the **s-wedge** derived from the set of **b-wedges** is a reasonable predictor of uncertainty as long as the *range* of oceanographic conditions remains similar from day to day. As a counterexample, if the range of conditions (and their impact on accuracy) varied dramatically between spring tides and neap tides, then one might achieve more accurate uncertainty estimates by performing such an analysis twice: once during spring tides and again during neap tides. By differing the parameters of the sub-sampling experiment, e.g., the number of casts per day or location, one can objectively seek a sampling regime which balances an increase in uncertainty against gains in survey efficiency through a hard cap on the number of casts to be collected. It is not the intention of this work to find such an optimal sampling scheme, but instead to demonstrate how such a scheme could be sought using the methods described herein.

We begin by quantifying the reduction in potential uncertainty achieved through the use of the MVP200. This is done by sequentially comparing each cast to its predecessor in the set, yielding 223 **b-wedges**. Each **b-wedge** represents the bias that affects the soundings at the moment just prior to collection of each cast. By compiling the **b-wedges** into an **m-wedge** and **s-wedge** (see Figure 24), one can ascertain the reduction in potential uncertainty gained through the use of the MVP system. In the well mixed, macro-tidal environment in Advocate Bay it is obvious that 224 casts provided more than enough information: the depth uncertainty of the outermost beam is approximately 4 cm in 40 m of water, well within the most stringent of survey specifications and a marked improvement over the potential uncertainty of roughly 12 cm as depicted in the **v-wedge** of Figure 23.

Would a single cast have done just as well? A similar analysis procedure is followed in which 223 **b-wedges** are computed by comparing each cast in the set to the very first cast of the set, i.e. there exist 223 cases where one can numerically quantify the bias that would occur if the first cast had been used for the entire survey. Compiling an **m-wedge** and **s-wedge** quantifies the average bias the data set would have suffered, as well as the dispersion of the soundings about the average bias (see Figure 25). In this case, using the first cast of the day would have introduced a significant average bias (see Figure 25a) and would have suffered the full

effects of the environmental variability (compare the **s-wedge** of Figure 25b to the **v-wedge** of Figure 19). Using the uncertainty wedges of Figure 25 as a lookup table, the outermost beam in 40 m of water would have been biased, on average, by approximately 0.10 m +/- 0.13 m. This is still quite tolerable in the water depths encountered in the survey area and with the 200% coverage typically achieved with CHS survey line spacing.

Although averaging **b-wedges** provides a useful “snapshot” of the potential uncertainty associated with a particular sampling regime, it masks potentially interesting details one may see by examining all of the **b-wedges** that went into the average. A useful way to visualize patterns and assess causes of bias is to geographically map the outermost beam bias at full depth for every **b-wedge**, as in Figure 26. In this case, the spatial variability in temperature and salinity has the potential to cause up to 25 cm of bias in the outermost beams had the first cast of the data set been used throughout the entire area.

Though the single cast proved tolerable in terms of sounding bias, the situation can be improved with use of only a few more casts. As the variability is primarily spatial in nature and does not exhibit complex spatial patterns, it may be preferable to simply “box in” the survey area with a few casts along the perimeter. For this example, we have chosen six casts, three along the southern perimeter and three along the northern perimeter. Each cast in the entire set of casts is compared to its nearest neighbour from the subset of six perimeter casts, generating 217 **b-wedges**. An **m-wedge** and an **s-wedge** for this particular sampling regime is shown in Figure 28. Mapping the outermost beam bias for this scenario demonstrates that this method yields much less bias than the case of a single cast as was examined previously (refer to Figure 27).

The pre-analysis effort yields a few hints on how to survey in such an area, assuming of course that conditions remain similar at other times. Variability is not significant and is primarily spatial in nature. A few well chosen cast locations could have significantly improved upon the potential bias introduced through the use of a single cast, even though a single cast provides reasonable accuracy over the range of water depths in the survey area.

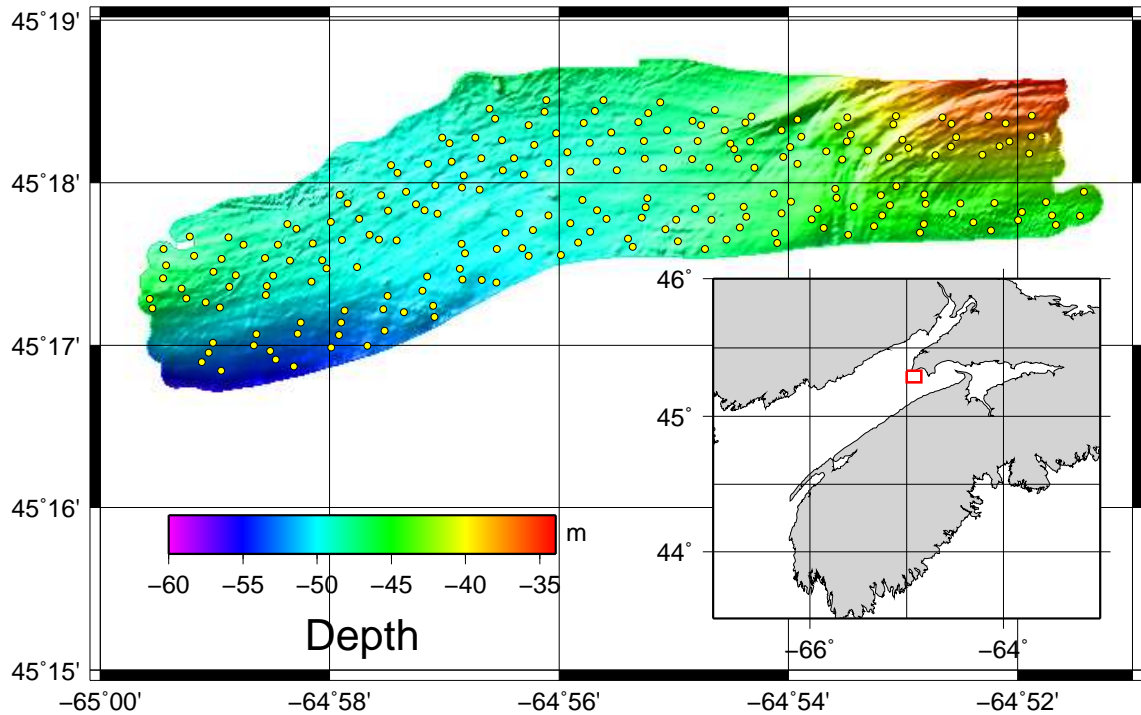


Figure 20: Survey area covered by CCGS Matthew during MVP200 data acquisition (224 casts, marked by yellow circles).

4 Application and Integration

4.1 Integration into CUBE

CUBE [5] is a computer-assisted hydrography algorithm that attempts to estimate the true depth at any given position within the survey area, and provide some guidance to the user as to how well that depth is known; CUBE is an acronym for “Combined Uncertainty and Bathymetry Estimator”. The essence of the CUBE algorithm is the understanding, modeling and utilisation of the uncertainty of the measurements that go into the depth soundings that are collected by MBES equipment; for dense MBES data, CUBE can provide very rapid, robust depth estimates from raw data and assist the user in assessing which data needs attention, improving the data workflow.

While CUBE itself does not mandate how uncertainties are computed for the soundings that it ingests, it does require that the uncertainties are “reasonable”

in the sense that they need to reflect at least a first-order accurate depiction of the actual variability of the soundings for the algorithm to operate as intended. Integration of the current work into CUBE therefore requires that we address the problem of how to integrate the uncertainty due to SSP spatio-temporal effects into the computation of the TPU, and consider the implications that this has for CUBE’s operation.

During development of the algorithm, the Hare-Godin-Mayer [9] model was used to construct TPU estimates for the soundings, and although the model has been refined since, it is still the most commonly used model for TPU estimation in current use. In this model, the effects of sound speed uncertainty are contained in terms that affect the fundamental uncertainties of range and angle estimation. Due to the paucity of information about the degree of spatio-temporal uncertainty at the time, however, the effects of measurement uncertainty in the SSP and the spatio-temporal variability of the watermass as reflected in the profile

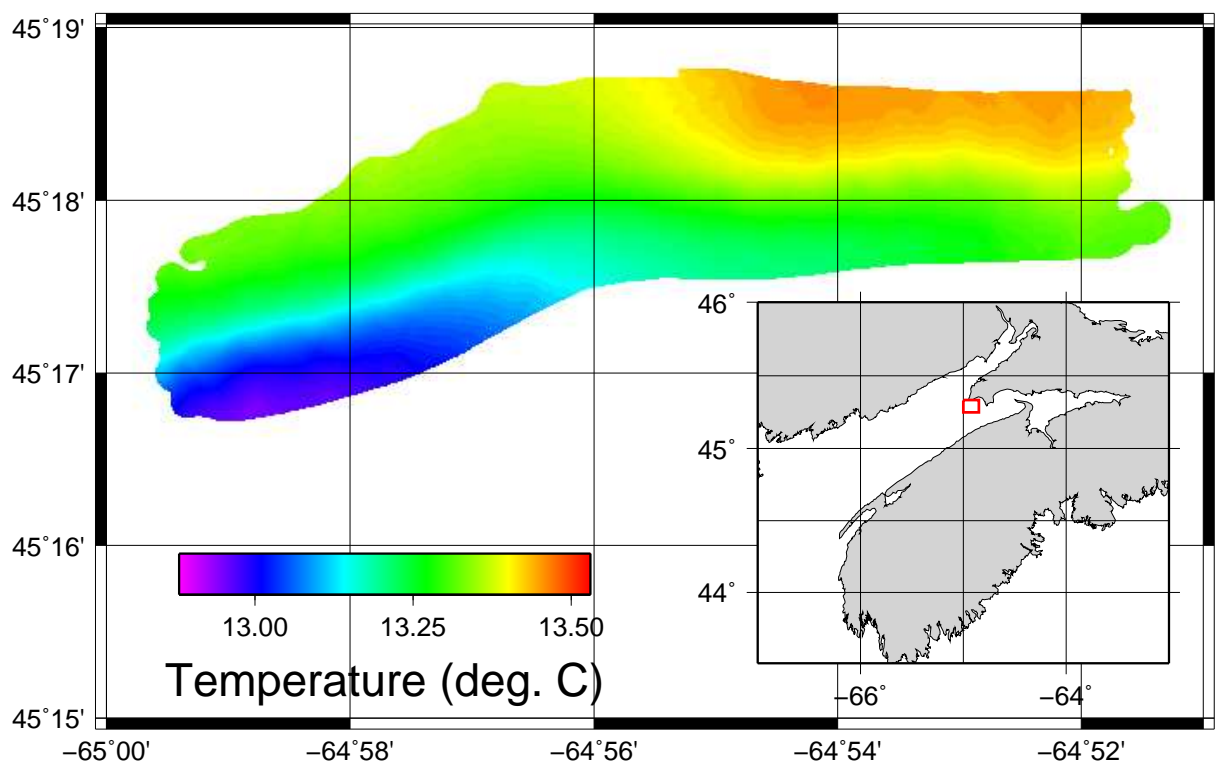


Figure 21: Map of temperature variation over survey area at 20 m water depth.

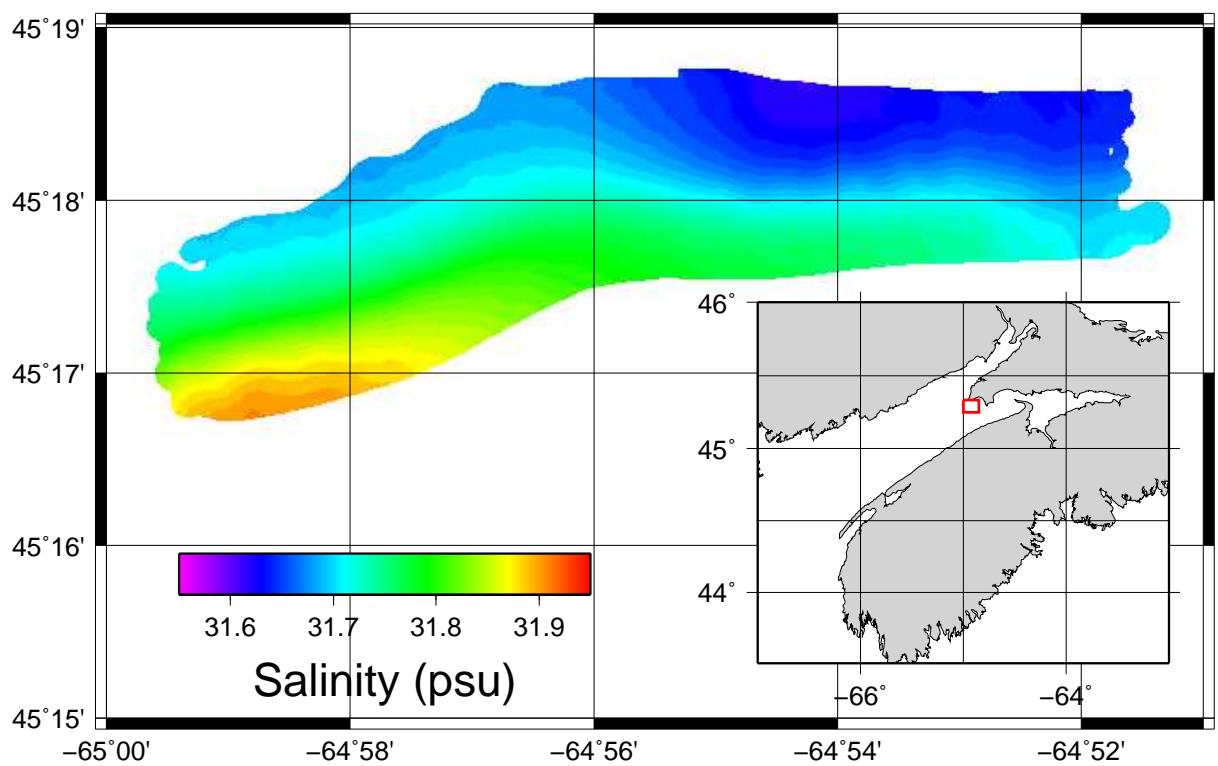


Figure 22: Map of salinity variation over survey area at 20 m water depth.

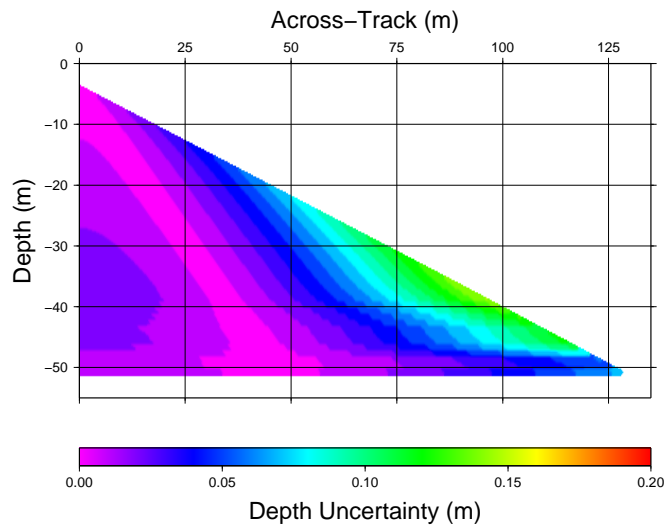


Figure 23: A **v-wedge** showing the potential uncertainty in the survey area. Note that the jagged appearance in the lower portion of the **v-wedge** is due to the decreasing number of casts at depths greater than 35 m. As fewer and fewer casts are available for the analysis at these depths, the standard deviation drops significantly as compared to the shallower sections of the watercolumn.

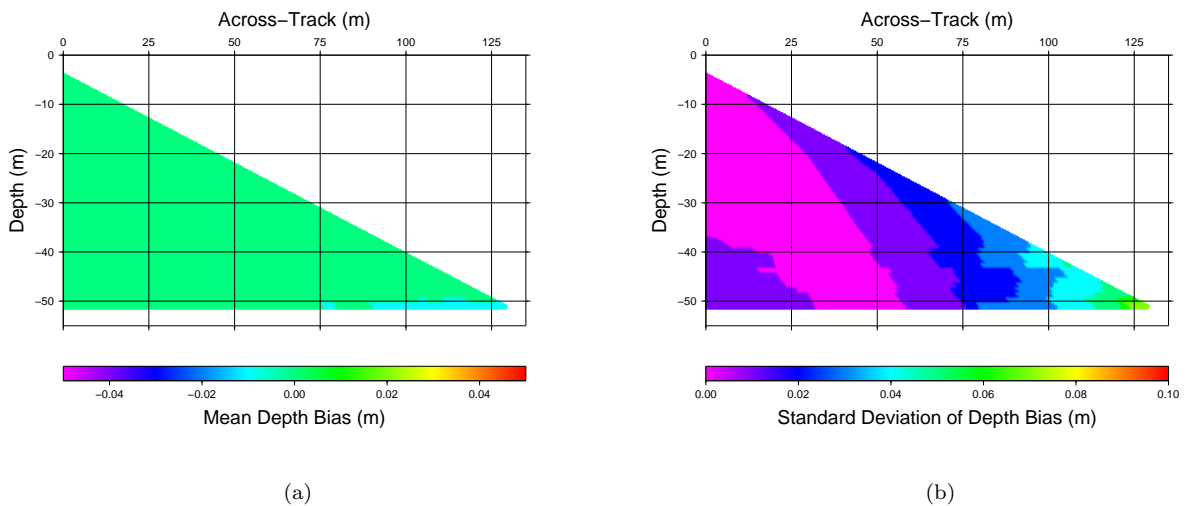


Figure 24: **M-wedge** and **s-wedge** showing uncertainty associated with using the entire set of casts. As with the **v-wedge** of Figure 23, the deeper portions of the wedges suffer from sharp discontinuities as the number of **b-wedges** contributing to the analysis for a given depth level declines with depth. In these cases, the shallower casts (and the **b-wedges** that result from comparison to short casts) do not contribute and the sample mean and standard deviation suddenly lock on to the potentially much tighter distribution of the deeper casts in the set.

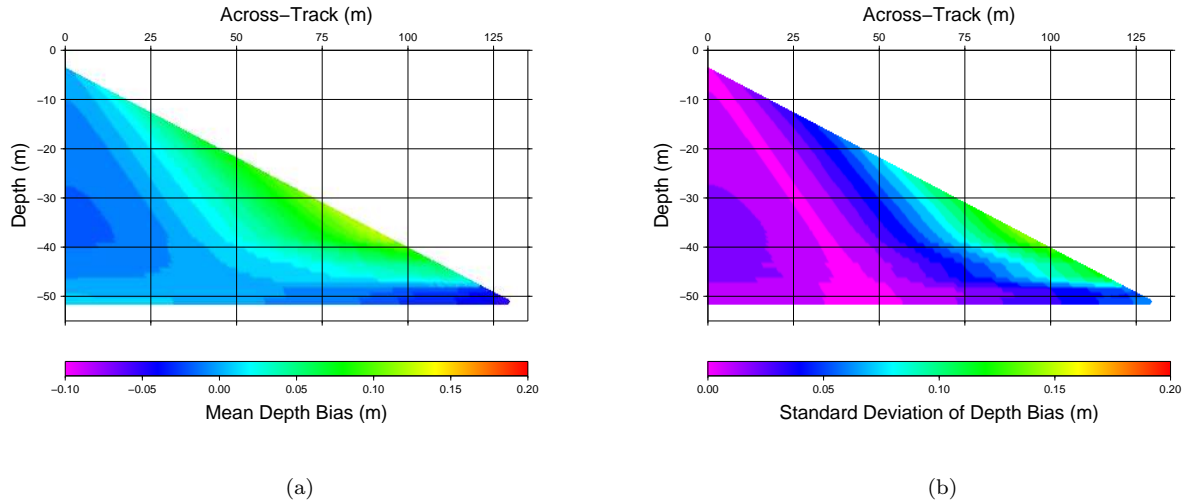


Figure 25: **M-wedge** and **s-wedge** showing uncertainty associated with using the first cast of the set instead of the 224 measured casts.

were combined into a single uncertainty term resulting in a simpler computational model, but a cruder representation of the true effects of the oceanographic environment. In particular, in environments where there is significant spatial specificity to the degree of SSP variation, the model is forced to adopt a pessimistic uncertainty analysis in order to cover the worst-case areas, and provides little assistance in assessing the effects for the user. This also results in reduction of processing power in CUBE since much of the algorithm's ability to determine likely depth reconstructions (which is essential to the efficiency of the algorithm) is predicated on the uncertainty reflecting the true nature of the soundings. By adopting a pessimistic analysis, the robustness of the estimation is weakened everywhere.

We now have the opportunity to refine this model through use of the UWA to reflect the spatio-temporal uncertainty. The current model represents the depth of the sounding by

$$\begin{aligned} d &= r \cos(\theta + \rho) \cos \phi \\ &= r \cos(\theta') \cos \phi \end{aligned} \quad (1)$$

with indicated range r and angle θ , roll ρ and pitch ϕ . (In the following, we work with the combined angle θ' for simplicity of presentation.) Using the principle of propagation of uncertainty, the predicted uncertainty in depth is

$$\sigma_d^2 = \left(\frac{\partial d}{\partial r}\right)^2 \sigma_r^2 + \left(\frac{\partial d}{\partial \theta'}\right)^2 \sigma_{\theta'}^2 + \left(\frac{\partial d}{\partial \phi}\right)^2 \sigma_\phi^2. \quad (2)$$

Pitch and roll are unaffected by SSP effects, but if we

trace the effects due to range and angle uncertainty through the vertical model, we find that they are, respectively

$$\sigma_{d(r)}^2 = \cos^2 \phi \cos^2 \theta' \sigma_r^2 \quad (3)$$

$$\sigma_{d(\theta)}^2 = r^2 \sin^2 \theta' \cos^2 \phi \sigma_{\theta'}^2 \quad (4)$$

and that the effects of the various components of uncertainty in range and angle are linear once multiplied by their respective sensitivity factors [12]. Knowing that Hare *et al.*[9] show that the uncertainty of range and angle measurement associated with SSP effects can be approximated as

$$\sigma_{r(\text{SSP})}^2 = \left(\frac{r}{v}\right)^2 \sigma_{v(\text{SSP})}^2 \quad (5)$$

$$\sigma_{\theta(\text{SSP})}^2 = \left(\frac{\tan \theta'}{2v}\right)^2 \sigma_{v(\text{SSP})}^2 \quad (6)$$

respectively, we can refactor (3) and (4) to extract the SSP specific terms, and evaluate the remainder of the model as at present. Specifically, if we assume that

$$\sigma_{v(\text{SSP})}^2 = \sigma_{v(\text{SSP-M})}^2 + \sigma_{v(\text{SSP-ST})}^2 \quad (7)$$

for measurement and spatio-temporal effects respectively, we can substitute in (5) and (6), extract the spatio-temporal component and develop a modified formulation that replaces the SSP spatio-temporal terms with the output of the UWA look-up tables, neglecting the terms

$$\sigma_{d(\text{SSP})}^2 = \frac{1}{4} (4 \cos^4 \theta' + \sin^4 \theta') \frac{r^2 \cos^2 \phi}{v^2 \cos^2 \theta'} \sigma_{v(\text{SSP-ST})}^2. \quad (8)$$

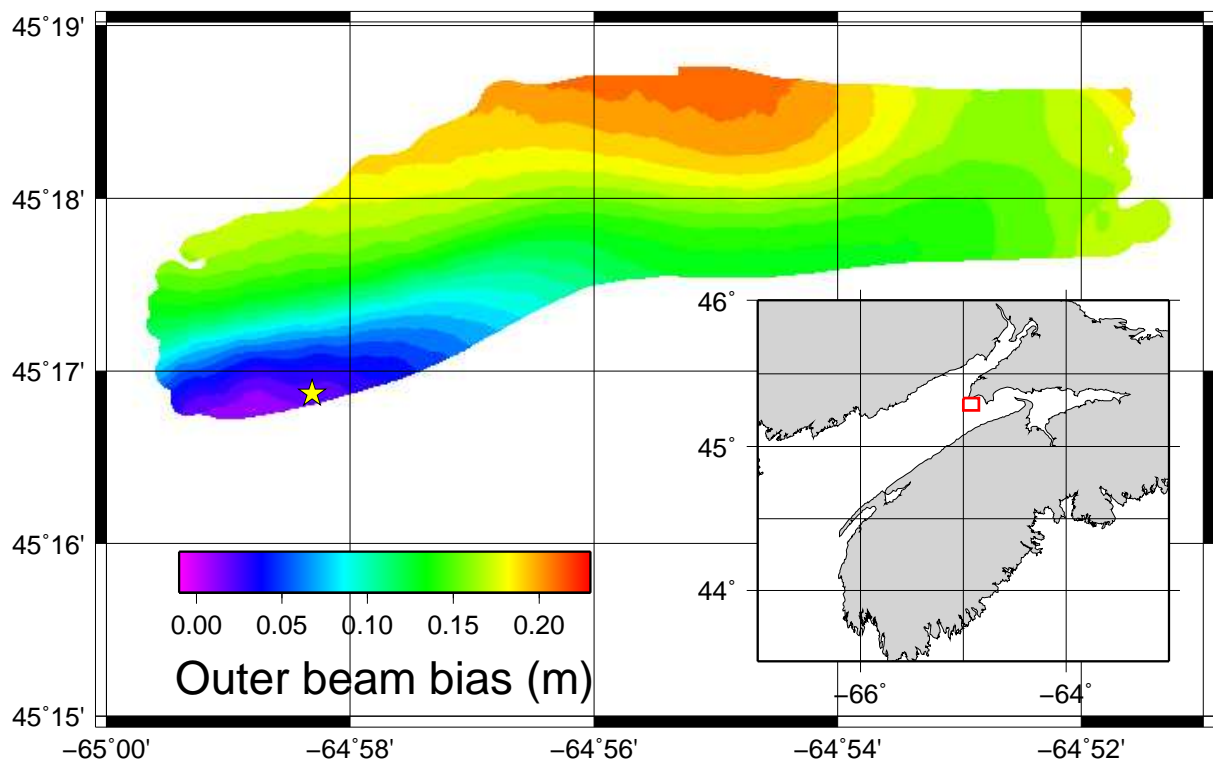


Figure 26: Map of outer beam bias experienced when using the first cast of the survey for the entire survey area (location of first cast marked by yellow star).

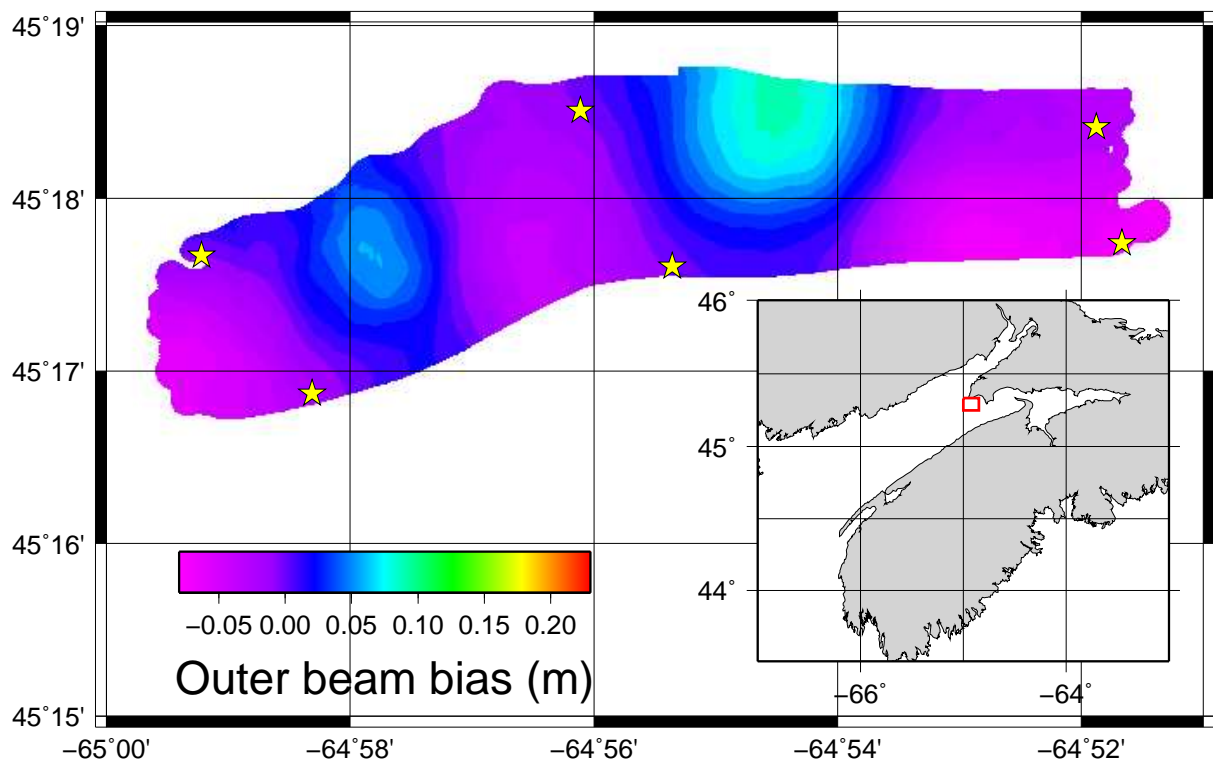


Figure 27: Map of outer beam bias experienced when using six casts along the perimeter of the survey area (locations marked by yellow stars). As expected the bias grows with distance from the cast locations.

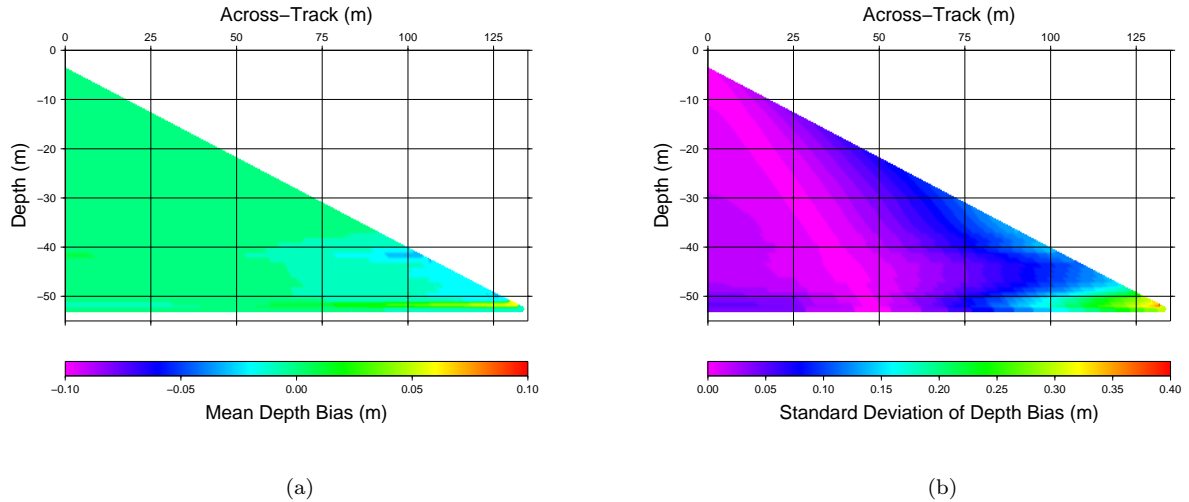


Figure 28: **M-wedge** and **s-wedge** showing uncertainty associated with using six casts on the perimeter instead of the 224 measured casts.

in the vertical and

$$\sigma_{p(\text{SSP})}^2 = \left(\frac{r}{v}\right)^2 \sigma_{v(\text{SSP-ST})}^2 \times \left[\left(1 - (\cos \theta' \cos \phi)^2\right) + \frac{1}{4} \left(1 - (\sin \theta' \cos \phi)^2\right) \tan^2 \theta' \right] \quad (9)$$

in the horizontal from the original model. In practice, this can be done simply by setting the value of $\sigma_{v(\text{SSP})}^2$ used at present to represent only the measurement uncertainty of the SSP component, and then adding the UWA-derived look-up table values in vertical and horizontal to the output of the current model.

A less ideal, but simpler to implement, solution would be to compute an estimate of the combined uncertainty per the original model by equating (8) and (9) for $\sigma_{v(\text{SSP-ST})}^2$ first and then combining the values with the measurement uncertainty for the SSP instrument using (7) before evaluating the model as currently implemented. This might be useful where the UWA shows that there is little need to re-evaluate the look-up tables per beam, since this approximation would provide a significant time saving in the computation.

There are three main implications for this technique applied to the CUBE algorithm. First, allowing the TPU algorithm to properly reflect the uncertainty of the SSP in the individual soundings should greatly assist the CUBE algorithm in maintaining robustness throughout the survey area. A great deal of the power of the CUBE algorithm resides in its ability to automatically sepa-

rate groups of soundings that are mutually inconsistent, and his action relies on the uncertainties of the soundings reflecting the variability expected in them. With empirical estimates of uncertainty applied, the number of stray soundings that are incorporated into an internally consistent group should decrease, which will lead to better in-group depth estimates, and therefore less interaction on the part of the user.

Secondly (and an immediate corollary of the first implication), in areas where there are significant SSP spatio-temporal effects, the increase in uncertainty applied in the UWA encourages the algorithm to consider soundings that are refracted as “sufficiently similar” that they can be accommodated as one consistent group, therefore reducing the number of spurious secondary hypotheses on the actual depth that are formed. Reduction of the number of hypotheses that are formed makes it simpler for the algorithm to assess which is most likely, and improves the algorithm’s ability to choose the “right” hypothesis to report to the user. The efficiency with which the user can process data depends strongly on how often the algorithm can do this, so the improved uncertainty estimates should reduce operator time correspondingly.

Thirdly, the uncertainty that is assessed within the group of soundings that are combined to make the depth estimate reported to the user as the primary hypothesis will, under the proposed scheme, better reflect the actual uncertainty in the data. At present, if the soundings have higher uncertainty than predicted (e.g., due to refraction), the algorithm tends to make

secondary hypotheses. The choice of which assessment of uncertainty to report to the user from the CUBE algorithm has been subject to some debate, but is currently most often an estimate of the standard deviation of the soundings used to compute the hypothesis. Currently, therefore, the assessment within the secondary hypotheses will only reflect the uncertainty of one group of soundings in the area, typically those from one pass of the MBES, and therefore underestimates the actual uncertainty of the data in the area. In the proposed scheme, the increased uncertainty associated with the SSP spatio-temporal effects would cause soundings with higher refraction effects to be considered as one hypothesis (per the previous implication), and therefore the uncertainty reported to the user would be correspondingly higher. This more accurately quantifies the actual uncertainty of the data in the area, and should result in better modeling and assessment of the value of the data in the area for the surveyors and the end users. Note that this is not to say that the data is necessarily useless under these conditions: depending on the survey standards in effect, the surveyor might assess the data as adequate, even given the increased uncertainty reflected in the final output. The outputs of the algorithm will, however, better reflect reality.

Assessing the magnitude of the effects of the proposed scheme in CUBE processing is a non-trivial process, in great part because of the subjective nature of the operator-in-the-loop processing that is still required by any practical processing system. It is possible, however, to assess both the number of hypotheses that the algorithm generates over a particular area, and measure how often the human operator agrees with the assessment of which hypothesis the algorithm thinks is correct by measuring the number of rejected hypotheses after operator intervention. Correlating these terms with a mapping of the uncertainty predicted by the UWA might provide a semi-quantitative method to assess the utility of the proposed scheme, and we are actively pursuing this in current research.

4.2 Integration into NOAA Workflows

While the merits of the uncertainty wedge analysis are theoretically valuable in their own right, we understand that a pragmatic approach be simultaneously taken in order for its significance to be realized. NOAA's Office of Coast Survey has written a sound speed analysis toolkit—VelociPy—that incorporates some of the UWA and VA functionality of the UNB SVP Toolkit [4].

At the beginning of 2008 an early version of the VelociPy toolkit (named ESS) [10] was made available

to NOAA field units, offering them a variation of the **v-wedge** described in section 1. This first pass at VelociPy was used by test-and-development personnel seeking to maximize efficiency of their survey operations [17]. The current version of VelociPy implements the ability to do simple wedge analysis, calculating a **v-wedge** for a set of profiles, calculating **b-wedges** between profile pairs, temporal scatter plotting of profiles and other tools that give the field hydrographer better oceanographic information. It is hoped that the current version of the VelociPy toolkit will allow field units to use UWA to better dynamically analyze the spatio-temporal variability of the sound speed in their project area and react accordingly to this new source of information.

NOAA's hydrographic survey workflow has yet to adjust to the new tools and techniques available and will now have several prospective options similar to those described above and by Beaudoin at Shallow Survey 2008 [1].

- NOAA may now have the ability to save on excess 'wear and tear' of profiling sensors and related equipment (e.g. moving vessel profiler fitted with a sound speed sensor) by using a **b-wedge** to determine whether the current sampling regime is sufficient or if oversampling is occurring. If water column features correlate to tidal activity then periodic checks once or twice a day may suffice. If the variability is occurring from multiplicative factors, then more consistent sampling and **b-wedge** analysis may be needed. The point is that the sampling rate may be adjusted on-the-fly.
- Likewise NOAA may be able to determine where more sound speed samples are necessary and in what approximate geographic location.
- These new additions may also be used during the project development stage using historical data. While it is possible that sound speed data is similar enough to weather in that there are no absolutes in determining exactly where a sample needs to be taken. However, by analyzing past variability and driving oceanographic factors, project managers may be able to instruct the field surveyors as to where an area has typically needed more sampling (or less).

In the upcoming field season, NOAA will be looking at simple test bed areas for the software testing and training purposes, then following with a few more complicated areas the next season to refine our practices.

5 Conclusion

Having the tools to assess this type of sensitivity in the field can help surveyors to make better decisions regarding temporal and spatial sound speed profile sampling. Oceanographic pre-analysis campaigns can be undertaken in areas where repetitive, high accuracy, surveys are the norm for safety of navigation or security.

The most important benefit of this approach is that uncertainty is estimated from watercolumn conditions directly, circumventing the problem of oversimplifying the water column in a model. As the uncertainty wedge representation provides estimates of uncertainty for each sounding based on its unique depth and across-track position in the potential sounding space, it has the potential to augment the fidelity of the water column variability component of uncertainty models used in the hydrographic community.

6 Future Work

6.1 Integration with Ocean Modeling

These new analytical techniques have given hydrographers the ability to better understand ocean variability and have greatly improved how NOAA can adjust sound speed sampling frequency. However, certain areas have such significant variability which are either impossible to capture or resource restrictions may prevent the use of a representative sampling regime that there may never be enough data to fully understand ocean dynamics.

For this reason, NOAA is supplementing the investigation of this technique with a model-based approach for predicting the level of variability in a survey area [11]. Rutgers University's ROMS numerical ocean circulation, forecast model has been used successfully to model shallow waters where a significant portion of NOAA hydrography occurs. For areas where a halocline or thermocline creates problems for multibeam systems, the model's horizontal and vertical grid resolution can be adjusted to capture the necessary physics associated with the area. Also, any additional post-processing metric requirements can be computed via Fortran routines and added to the existing ROMS software package.

NOAA is currently developing operational circulation/forecast models for Chesapeake Bay, Tampa Bay, and Delaware Bay and has future hopes of completing a model for Cook Inlet, AK.

For surveys which fall within areas for which there exist validated ROMS models, we envision the models

to be used during the survey planning process. During survey planning, output of the model may predict the driving factors of the local oceanography, allowing the determination of an appropriate sampling regime. ROMS includes the ability for data assimilation, so a typical first day of surveying may include oversampling the water column profiles for the purposes of model validation.

The caveat of this approach is that producing an operational ROMS model for each particular geographical area can take an extended duration (especially if data is not readily available) and requires a great amount of resources. However, once the model is validated, it may run in perpetuity. For this reason the region-by-region predictive modeling approach for creating a sound speed sampling regime may have limited application, until a larger basin-scale set of oceanographic models can be developed and validated.

6.2 UWA and VA with sparse data sets

Though the value of this new method of estimating uncertainty due to refraction is attractive, it relies heavily on having an oversampled watermass, something which is not always practical to collect. The question then becomes: can this be done, or at least approximated, with an undersampled watercolumn only? Future work will investigate whether UWA and VA gives reasonable results when given much smaller data sets of casts. Of course both methods can provide results with small data sets, but how uncertain are we willing to be about our uncertainty?

7 Acknowledgments

This work was supported by the sponsors of the OMG and by NOAA under grant NA05NOS4001153. The authors would like to thank Rijkswaterstaat for the opportunity to participate in the Rotterdam Waterway trial as it provided the perfect data set for which to showcase the analysis methods presented in this work. The Canadian Hydrographic Service is thanked for acquiring the Advocate Bay data set on our request. Thank you to Dr. Lyon Lanerolle for his supporting work with the ROMS ocean circulation model and for reviewing the related sections of this article.

References

- [1] J. D. Beaudoin. Real-time monitoring of uncertainty due to refraction in multibeam echosounding. In *Proc. Shallow Survey 2008*, Oct 2008.

- [2] J. D. Beaudoin, J. E. Hughes Clarke, and J. Bartlett. Application of surface sound speed measurements in post-processing for multi-sector multibeam echosounders. *International Hydrographic Review*, 5(3), 2004.
- [3] J. D. Beaudoin, J. E. Hughes Clarke, and J. Bartlett. Usage of oceanographic databases in support of multibeam mapping operations on-board the CCGS Amundsen. *Lighthouse, Journal of the Canadian Hydrographic Association*, (68), 2006.
- [4] J. D. Beaudoin, J. E. Hughes Clarke, J. Bartlett, S. Blasco, and R. Bennett. Mapping canada’s arctic seabed: Collaborative survey processing and distribution strategies. In *Proc. Canadian Hydrographic Conference 2008*, May 2008.
- [5] B. R. Calder and L. A. Mayer. Automatic processing of high-rate, high-density multibeam echosounder data. *Geochem., Geophys. and Geosystems (G3) DID 10.1029/2002GC000486*, 4(6), 2003.
- [6] D. S. Cartwright and J. E. Hughes Clarke. Multi-beam surveys of the frazer river delta, coping with an extreme refraction environment. In *Proc. Canadian Hydrographic Conference 2002*, May 2002.
- [7] D. F. Dinn, B. D. Loncarevic, and G. Costello. The effect of sound velocity errors on multi-beam sonar depth accuracy. In *Proc. IEEE Oceans 1995*, volume 2, pages 1001–1010. IEEE, Oct 1995.
- [8] E. Hammerstad. Multibeam echo sounder accuracy. Technical report, Kongsberg Maritime AS, 2001.
- [9] R. Hare, A. Godin, and L. A. Mayer. Accuracy estimation of canadian swath (multibeam) and sweep (multitransducer) sounding systems. Technical report, Canadian Hydrographic Service, 1995.
- [10] G. Imahori and J. Hiebert. An algorithm for estimating the sound speed component of total depth uncertainty. In *Proc. Canadian Hydrographic Conference 2008*, May 2008.
- [11] G. Imahori, L. Lanerolle, S. Brodet, R. Downs, J. Xu, R. Becker, and L. Robidoux. An integrated approach to acquiring sound speed profiles using the Regional Ocean Modeling System (ROMS) and an Autonomous Underwater Vehicle (AUV). In *Caris Conference*, 2008.
- [12] International Organisation for Standardization. Guide to the expression of uncertainty in measurements. Technical report, ISO, Geneva, 1995. ISBN 92-67-10188-9.
- [13] Kongsberg Maritime AS. *Operators Manual - EM Series Datagram Format (20-01-06)*, 2006.
- [14] H. Medwin and C. S. Clay. *Fundamentals of Acoustical Oceanography*. Academic Press, 1998.
- [15] National Oceanic and Atmospheric Administration. *NOS Hydrographic Surveys Specifications and Deliverables*, 2008.
- [16] Reson Inc. *SeaBat 8101 Multibeam Echosounder System Operators Manual Version 2.20*, 2000.
- [17] D. Wright. Analysis of NOAA methods of application of sound speed uncertainty and alternatives derived from use of the Estimating Sound Speed uncertainty software. In *Proc. Shallow Survey 2008*, Oct 2008.

A Raytracing Simulator Functionality

In order to serve as a reasonable predictor of sounding uncertainty, the simulator must honour the real-time sounding geometry as much as possible. The raytracing procedure thus requires reasonable estimates of several parameters, some of which simply modify the range of depths and angles to be investigated whereas others fundamentally change the behaviour of the raytracing algorithm. These are listed below along with explanation of how they affect the fidelity of the simulation.

Surface speed probe. A surface sound speed probe is often required to ensure correct electronic beam steering angles with linear transducer arrays. It is also often used to augment the sound speed profile during raytracing by (1) using the measured surface value as “the initial entry in the sound speed profile used in the raytracing calculations” [13] or (2) calculating Snell’s constant, or the ray parameter, with the observed surface value prior to raytracing [2]. As pointed out by Cartwright and Hughes Clarke [6], the incorporation of the surface sound speed measurement has a significant effect on the behaviour of a raytracing algorithm, in some cases it allows for a graceful recovery from surface layer variability as long as the deeper portion of the watermass is relatively invariant. Regardless of this potential gain, the inclusion of the

surface sound speed as an additional measurement fundamentally changes the behaviour of a raytracing algorithm thus its effect must be included in uncertainty models.

The UNB method mimics the use of a surface sound speed probe by retrieving the sound speed at transducer depth from the reference profile and using this to compute the ray parameter for the test cast raytrace without modifying the test cast (i.e. replacing the measurement at the draft depth with the surface sound speed). One must take care, however, to only perform this additional step if the acquisition and/or post-processing software can accommodate the surface sound speed as an additional aiding measurement during sounding reduction, specifically the raytracing portion of the procedure. For example, a surface sound speed value may be input into a Reson 8101 MBES for use in pitch stabilization [16]. Though this value is logged in the data stream, it is not used in subsequent raytracing calculations performed in post-processing in Caris HIPS (Wong, personal comm.). In this case, the simulator should not be configured to mimic a surface sound speed probe as this would give inaccurate results, especially in the case where surface variability is significant.

Angular sector. The nominal angular sector that can be achieved by the sounder controls the shallowest depression angle that must be investigated and heavily influences a mapping systems overall sensitivity to variable watercolumn conditions. As the outermost edges of the swath are typically the most sensitive to refraction, the predictive ability of the simulator depends heavily on having an accurate estimate of the outermost beams depression angle. The outermost depression angle can be easily underestimated and overestimated in various conditions. These two cases are examined in turn below.

In dynamic roll conditions, a system that is not roll-stabilized can experience larger refraction artifacts in the outer portions of the swath due to smaller than normal depression angles associated with extremes in vessel roll. By limiting the investigation to the nominal angular sector, the simulator would underestimate the refraction in the outermost beams during large roll events and the output would be overly optimistic (though this would only apply to one side of the swath). If the outermost soundings must be retained to maintain overlap between survey lines, then the simulator should allow for an artificial increase to the angular sector to allow for large roll events. It should be noted that in particularly large roll events ($10^\circ - 15^\circ$) and with large angular sector systems (e.g. $\pm 75^\circ$), the outermost rays will tend to horizontal and will not

likely have a bottom return. With an unstabilized system, the operator must make an effort to estimate the largest achieved angular sector instead of simply increasing the angular sector by adding the largest expected roll value. Vessel pitch can also reduce the outermost depression angles though the influence is not nearly as pronounced as that of vessel roll.

In the case that the outermost edges of the swath fall beyond the maximum achievable range of a mapping system, the achieved angular sector can be significantly smaller than the nominal case. In this case, the simulator must allow for a reduction of angular sector with increasing depth, otherwise the uncertainty estimates would be overly pessimistic. This can be done manually by adjusting the angular sector to match the sector achieved under actual working conditions. This would also apply in the case where filtering applied in post-processing would artificially reduce the angular sector, e.g. filtering all soundings outside of $\pm 60^\circ$.

Draft. A particular mapping system's susceptibility to surface variability can vary dramatically depending on the depth of the transducer in the watercolumn. The transducer draft should therefore be used as the start point of the raytrace. The simulator currently does not allow for vertical motion of the transducer through the watercolumn and all analyses are based on a static draft assumption.

B Simulation of Surface Sound Speed Probe

Variability Analysis (VA) is based upon examining the divergence of a bundle of raypaths, with each raypath tied to a different depiction of the watercolumn. For a given travel time, depression angle and surface sound speed, the bundle of rays will land at some location in the potential sounding space. The scatter of their solutions about their mean position in the potential sounding space serves as an indicator of the sensitivity to watercolumn variability. The problem is that we need to simulate the use of a common surface sound speed measurement as the initial entry into the watercolumn during the raytrace for each ray in the bundle, but which sound speed should be used? It turns out that it doesn't matter.

Consider a raytrace with a depression angle of 20° (incidence angle of 70°) and sound speed of 1445 m s^{-1} . The ray parameter used in the raytrace is calculated as:

$$k_1 = \sin(70^\circ)/1445$$

As the ray parameter is a function of depression an-

gle and sound speed, there exists other angle/sound speed pairs that would yield the same rayparameter. For example, consider a surface sound speed of 1440 m s^{-1} . Snell's law is applied to determine which angle would give the same ray parameter:

$$\begin{aligned}
 k_2 &= \sin(\theta)/1440 = k_1 \\
 \Rightarrow \sin(\theta)/1440 &= \sin(70^\circ)/1445 \\
 \text{so: } \theta &= \arcsin(1440 \sin(70^\circ)/1445) \\
 &\approx 69.462^\circ \\
 \therefore \psi &= 90^\circ - \theta \approx 20.538^\circ
 \end{aligned}$$

where ψ is the depression angle.

If one were to perform an acoustic raytrace with a common sound speed profile and differing surface sound speed/depression angle pairs, the rays would share the exact same raypath, despite having different depression angles and different surface sound speeds. In essence, it is possible to get to the same location on the seafloor through a different launch angle and surface sound speed combination.

How does this apply to the simulation of the use of a surface sound speed probe in VA? If the above exercise is true for one ray, then it is true for all rays in a bundle of rays being investigated in a VA. One can arrive at the mean location by investigating a given depression angle and surface sound speed from one of the casts, or by using a different depression angle and a different surface sound speed, chosen from a different cast in the set. As all of the rays in the bundle will all arrive at their same respective positions in either case, then their relative positions with respect to their mean position will remain the same. It follows that the dispersion of the solutions about the mean location would also remain the same regardless of how the bundle of rays arrived at the mean location. In other words, any one of the casts can be chosen as a measurement of truth and we would eventually, through some combination of surface sound speed and depression angle, arrive at the same mean location and witness the same dispersion of the raytraced solutions. So, an arbitrary surface sound speed value could be chosen, and with a systematic sweep across the angular sector we will have visited every spot in the potential sounding space and calculated the dispersion in the same manner had another surface sound speed been chosen.

Note that the exact matching of raytraced solutions depends heavily on how the raytrace algorithm uses the additional surface sound speed measurement to augment the sound speed profile. The following procedure is used with the UNB method: (1) the surface sound speed and depression angle are used to define the ray

parameter, and (2) the ray is immediately refracted at the beginning of the raytrace as if an infinitesimally thin layer of water exists at the transducer face in which the speed of sound is the measured surface sound speed.

Deviation from this methodology will result in small discrepancies in the equality of a ray solutions when one modifies the surface speed or depression angle as we have in this exercise. For example, simply replacing the sound speed at the transducer depth in the watercolumn can yield slight inconsistencies in the results and is sensitive to layer thickness in the raytrace algorithm.